



LUND UNIVERSITY

Comparative analysis of the effects of neurotrophic factors CDNF and GDNF in a nonhuman primate model of Parkinson's disease

Garea-Rodríguez, Enrique; Eesmaa, Ave; Lindholm, Päivi K; Schlumbohm, Christina; König, Jessica; Meller, Birgit; Krieglstein, Kerstin; Helms, Gunther; Saarma, Mart; Fuchs, Eberhard

Published in:
PLoS ONE

DOI:
[10.1371/journal.pone.0149776](https://doi.org/10.1371/journal.pone.0149776)

2016

[Link to publication](#)

Citation for published version (APA):

Garea-Rodríguez, E., Eesmaa, A., Lindholm, P. K., Schlumbohm, C., König, J., Meller, B., Krieglstein, K., Helms, G., Saarma, M., & Fuchs, E. (2016). Comparative analysis of the effects of neurotrophic factors CDNF and GDNF in a nonhuman primate model of Parkinson's disease. *PLoS ONE*, 11(2), 1-21.
<https://doi.org/10.1371/journal.pone.0149776>

Total number of authors:
10

General rights

Unless other specific re-use rights are stated the following general rights apply:
Copyright and moral rights for the publications made accessible in the public portal are retained by the authors and/or other copyright owners and it is a condition of accessing publications that users recognise and abide by the legal requirements associated with these rights.

- Users may download and print one copy of any publication from the public portal for the purpose of private study or research.
- You may not further distribute the material or use it for any profit-making activity or commercial gain
- You may freely distribute the URL identifying the publication in the public portal

Read more about Creative commons licenses: <https://creativecommons.org/licenses/>

Take down policy

If you believe that this document breaches copyright please contact us providing details, and we will remove access to the work immediately and investigate your claim.

LUND UNIVERSITY

PO Box 117
221 00 Lund
+46 46-222 00 00

RESEARCH ARTICLE

Comparative Analysis of the Effects of Neurotrophic Factors CDNF and GDNF in a Nonhuman Primate Model of Parkinson's Disease

Enrique Garea-Rodríguez^{1,2,3*}, Ave Eesmaa⁴, Päivi Lindholm⁴, Christina Schlumbohm^{1,5}, Jessica König^{1,5}, Birgit Meller⁶, Kerstin Kriegelstein⁷, Gunther Helms⁸, Mart Saarma⁴, Eberhard Fuchs^{1,3}



OPEN ACCESS

Citation: Garea-Rodríguez E, Eesmaa A, Lindholm P, Schlumbohm C, König J, Meller B, et al. (2016) Comparative Analysis of the Effects of Neurotrophic Factors CDNF and GDNF in a Nonhuman Primate Model of Parkinson's Disease. PLoS ONE 11(2): e0149776. doi:10.1371/journal.pone.0149776

Editor: David I Finkelstein, Florey Institute of Neuroscience and Mental Health, The University of Melbourne, AUSTRALIA

Received: January 20, 2015

Accepted: February 4, 2016

Published: February 22, 2016

Copyright: © 2016 Garea-Rodríguez et al. This is an open access article distributed under the terms of the [Creative Commons Attribution License](http://creativecommons.org/licenses/by/4.0/), which permits unrestricted use, distribution, and reproduction in any medium, provided the original author and source are credited.

Data Availability Statement: The authors confirm that all data underlying the findings are fully available without restriction. All relevant data are within the paper and its Supporting Information files.

Funding: EGR was funded by EU ERA-Net NEURON (PARKCDNF) (<http://www.neuron-eranet.eu/>). The study was partially supported by the DFG Research Center Molecular Physiology of the Brain (CMPB) (<http://www.cmpb.uni-goettingen.de/>) and by a S. Jusélius Foundation (<http://www.sigridjuselius.fi/foundation>) grant to MS. The funders had no role in

1 Clinical Neurobiology Laboratory, German Primate Center, Göttingen, Germany, **2** Department of Neuroanatomy Institute of Anatomy and Cell Biology, Albert-Ludwigs-University Freiburg, Freiburg, Germany, **3** Center for Molecular Physiology of the Brain (CMPB), University of Göttingen, Göttingen, Germany, **4** Institute of Biotechnology, University of Helsinki, Helsinki, Finland, **5** Encepharm, Göttingen, Germany, **6** Department of Nuclear Medicine, University Medical Center, Georg-August-University Göttingen, Göttingen, Germany, **7** Department of Molecular Embryology, Institute for Anatomy and Cell Biology, Albert-Ludwigs-University Freiburg, Freiburg, Germany, **8** Department of Cognitive Neurology, University Medical Center, Georg-August-University Göttingen, Göttingen, Germany

* enrique.garea.rodriguez@anat.uni-freiburg.de

Abstract

Cerebral dopamine neurotrophic factor (CDNF) belongs to a newly discovered family of evolutionarily conserved neurotrophic factors. We demonstrate for the first time a therapeutic effect of CDNF in a unilateral 6-hydroxydopamine (6-OHDA) lesion model of Parkinson's disease in marmoset monkeys. Furthermore, we tested the impact of high chronic doses of human recombinant CDNF on unlesioned monkeys and analyzed the amino acid sequence of marmoset CDNF. The severity of 6-OHDA lesions and treatment effects were monitored *in vivo* using ¹²³I-FP-CIT (DaTSCAN) SPECT. Quantitative analysis of ¹²³I-FP-CIT SPECT showed a significant increase of dopamine transporter binding activity in lesioned animals treated with CDNF. Glial cell line-derived neurotrophic factor (GDNF), a well-characterized and potent neurotrophic factor for dopamine neurons, served as a control in a parallel comparison with CDNF. By contrast with CDNF, only single animals responded to the treatment with GDNF, but no statistical difference was observed in the GDNF group. However, increased numbers of tyrosine hydroxylase immunoreactive neurons, observed within the lesioned caudate nucleus of GDNF-treated animals, indicate a strong bioactive potential of GDNF.

Introduction

Neurotrophic factors are considered potent candidates for the disease modifying treatment of neurodegenerative disorders such as Parkinson's disease (PD). The newly discovered cerebral dopamine neurotrophic factor (CDNF) gained attention because it restored function and

study design, data collection and analysis, decision to publish, or preparation of the manuscript.

Competing Interests: Authors Christina Schlumbohm and Jessica König are employed at the commercial company Encepharm. This does not alter the authors' adherence to PLOS ONE policies on sharing data and materials.

promoted survival of midbrain dopaminergic (DA) neurons in 6-hydroxydopamine (6-OHDA) and 1-methyl-4-phenyl-1,2,3,6-tetrahydropyridine (MPTP) models of PD in rodents when delivered intracranially either as a recombinant protein or with adeno-associated viral serotype 2 (AAV2) vector as treatment regimens in rodent models of PD [1–6].

CDNF and related protein mesencephalic astrocyte-derived neurotrophic factor (MANF) represent an evolutionarily conserved family of neurotrophic factors with a unique structure and mode of action [1], [7–10]. The CDNF amino acid sequence is found in vertebrates [1], whereas invertebrates have a single homolog more related to mammalian MANF than to CDNF [11]. The three dimensional structure of MANF/CDNF proteins consist of two domains [7, 9] and eight cysteine residues determining the domain folding are conserved across species. Although MANF/CDNF proteins can be secreted [1, 12] they also function in the endoplasmic reticulum (ER) and the protective role for MANF against ER stress has been demonstrated [13–15].

Glial cell line-derived neurotrophic factor (GDNF) has been considered the most promising neurotrophic factor, showing positive effects in several rodent and nonhuman primate models of PD [16–24], but by contrast with CDNF, it had very modest effects in a severe rat 6-OHDA model of PD [3]. Interestingly, GDNF had no neuroprotective effects in the severe alpha-synuclein (α -syn) model of PD [25–26], because α -syn downregulates transcription factor Nurr1 and consequently GDNF signaling receptor RET, disrupting GDNF signalling in DA neurons [27]. In PD patients, gene therapy using neurturin (NRTN), a member of the GDNF family ligands showed a modest clinical benefit compared to placebo controlled trials [28].

Controversial results from clinical trials with GDNF protein [29–32] and NRTN gene therapy have highlighted the importance of effective and reliable administration techniques (discussed by Sherer and colleagues [33]) [34–37]. Moreover, GDNF and NRTN are basic proteins that bind with high affinity to heparin sulfate proteoglycans in the extracellular matrix [38], which restricts their diffusion in the brain tissue [39]. We have recently shown that CDNF and MANF are neutral proteins that diffuse significantly better than GDNF in rodent brains [2–3]. These results together with CDNF efficiency to protect and repair DA neurons in rodent mid-brain warrant testing for its efficacy in nonhuman primate models of PD.

Nonhuman primates, e.g. common marmosets (*Callithrix jacchus*), share similarities with humans regarding complex brain function and drug safety. Potent compounds such as neurotrophic factors can cause undesired effects as reported for nerve growth factor (NGF) and GDNF when applied in high doses into the brain [40–42]. The present tolerability study aimed to define experimental parameters for a safe intracerebral application of CDNF protein in the future.

The impact of lesion severity on brain integrity and repair processes should be considered when studying neuroregeneration [43–48]. Of note, neuroprotective approaches were generally more successful than neurorestorative approaches [1, 22], and this fact may be attributed to the chronic neurodegeneration of DA neurons in the 6-OHDA model, especially after nigral and nigrostriatal bundle lesions [46, 49]. With regard to translational aspects, severe 6-OHDA lesions chiefly mimic the endpoint of Parkinson's disease, where the majority of DA neurons are lost and are therefore of limited use for therapeutic studies [46]. In our concept of a successful neurorestorative treatment approach, the endogenous regenerative capacity of the brain needs to be conserved. Consequently, establishing a 6-OHDA protocol for mild lesions in marmosets was required.

In the presented study we induced mild 6-OHDA lesions into the caudate nucleus of common marmosets as a preclinical model for neurodegeneration. The aim of the study was to test the therapeutic efficacy of CDNF and to compare it with GDNF in a neurorestorative treatment approach. Striatal DA neurodegeneration was monitored *in vivo* by following dopamine

transporter integrity using ^{123}I -FP-CIT SPECT. To provide an additional aspect on biosafety, we assessed the tolerability of high CDNF doses. Moreover, we determined the marmoset CDNF amino acid sequence and compared it within primates.

Materials and Methods

Ethics Statement

The animals were obtained from the breeding colony at the German Primate Center (Göttingen, Germany) and pair-housed in a temperature- ($25 \pm 1^\circ\text{C}$) and humidity-controlled ($65 \pm 5\%$) facility under a 12 h day/night cycle. Each cage (80 x 150 x 66 cm, Ebeco GmbH, Castrop-Rauxel, Germany) was furnished with wooden branches and shelves and contained a wooden sleeping box (24 cm x 21 cm x 18 cm). The animals were fed *ad libitum* with a pelleted marmoset diet (Ssniff Spezialdiäten, Soest, Germany). In addition, a mash which contains in the dry matter 21% crude protein, 14% fat, 10% crude fiber, 41% starch and saccharides, 0.95% and Ca, 0.67% was served in the morning. Per animal 20 g of the mash with a dry matter content of 38% was offered. In the afternoon each animal received 30 g clean-cut fruit or vegetables mixed with noodles or rice. Water was always available. Behavior of the animals was observed on a daily basis and their weight was measured every week. All animal experimentation was carried out in accordance with the European Council Directive of September 2010 (2010/63/EU), and was approved by the Lower Saxony Federal State Office for Consumer Protection and Food Safety, Germany (permit numbers: 04-076/09, 04-10/0161 and 04-11/0394).

Animals

Four adult male (3–4 years old) and two female (3 and 6 years old) common marmoset monkeys (*Callithrix jacchus*) (337–485g) were used for the chronic CDNF infusion study. Eight adult (3–7 years old) male and one female (9 years old) animal (375–550g) were used for the treatment study. One adult female (2 years old) animal was used for CDNF sequence analysis.

Chronic intracerebral delivery of CDNF

CDNF protein was chronically delivered into the right caudate nucleus via an implanted cannula connected to an osmotic pump. Surgery was carried out under inhalation anaesthesia [60:40 $\text{N}_2\text{O}:\text{O}_2$; isoflurane (0.5–1.5%)] and diazepam (Ratiopharm, Germany; 0.05 mg per animal) anaesthesia and aseptic conditions. A Teflon infusion cannula (PlasticsOne, Roanoke, VA, USA) was inserted stereotactically into the right caudate nucleus (AP+8.0 mm; L+3.0 mm, V+13.0 mm) according to the atlas by Stephan and colleagues [50]. After the injection cannula was inserted into the brain, it was fixed to the skull with dental cement. An Alzet osmotic mini-pump (model 2004, 0.25 $\mu\text{l}/\text{h}$; Charles River, Sulzfeld, Germany) was implanted subcutaneously in the retroscapular area and connected to the infusion cannula via the catheter tube to deliver either CDNF or 0.1 M phosphate buffered saline (PBS), pH 7.2 for a period of 4 weeks. Human recombinant CDNF was expressed and purified as previously described [1] with additional removal of tag sequences by thrombin cleavage. The pumps were filled with CDNF dissolved in PBS and 0.1% bovine serum albumin (BSA). As a control, pumps were filled with PBS and 0.1% BSA alone. Four animals received 15 μg CDNF per day (CDNF concentration 2.5 $\mu\text{g}/\mu\text{l}$, 6 $\mu\text{l}/24$ h), and one animal received 10 μg CDNF per day (CDNF concentration 1.7 $\mu\text{g}/\mu\text{l}$, 6 $\mu\text{l}/24$ h), chronically delivered for 4 weeks (Fig 1). Thus, one group of the animals received a total of 420 μg of CDNF and the other group 280 μg . A single animal received PBS as a control. Postoperatively, the animals were treated with meloxicam (0.2 mg/kg i.m., Metacam, Boehringer Ingelheim, Germany) for 3 days and enrofloxacin (5 mg/kg i.m., Baytril, Bayer, Germany) for 5 days.

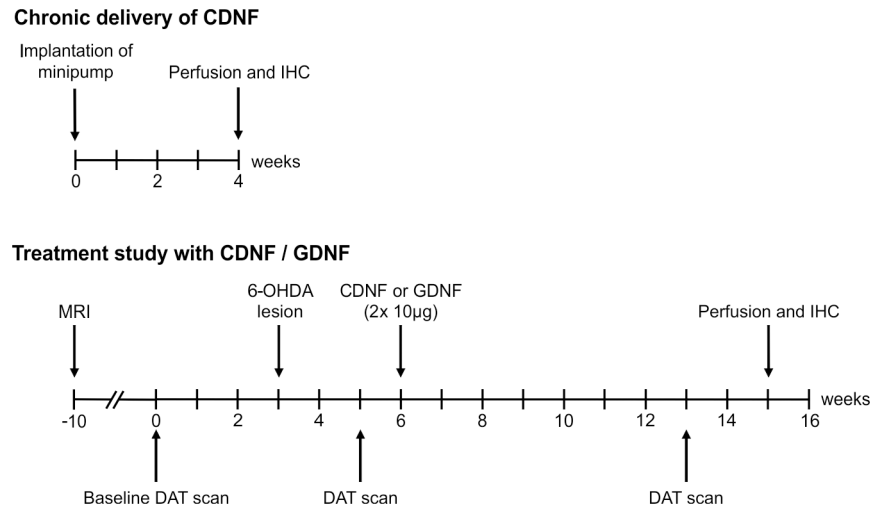


Fig 1. Time course of experiments. In the tolerability approach (upper scheme) high concentrations of CDNF (10 or 15 µg per day) were intrastrially delivered for 28 days via osmotic minipumps followed by subsequent histopathological assessment. Efficacy of CDNF and GDNF was tested in the 6-OHDA model (lower scheme). Treatment effects were evaluated *in vivo* by SPECT imaging and post mortem IHC.

doi:10.1371/journal.pone.0149776.g001

Mild unilateral 6-hydroxydopamine lesion and intracerebral injection of neurotrophic factors

Marmosets were given unilateral 6-OHDA injections into the caudate nucleus. Anesthesia was induced and maintained as described above. 6-OHDA (1.66 mg/ml free base weight 6-OHDA hydrobromide [Sigma-Aldrich, Steinheim, Germany] dissolved in 0.01% ascorbate-saline) was injected stereotactically into six sites (5.81 µg/3.5 µl each injection) within the caudate nucleus on one side of the brain. Coordinates were determined according to the atlas by Stephan and colleagues [50]: first site: AP+7.5 mm, L+2.5 mm, V+12.5 mm; second site: AP+7.5 mm, L+3.5 mm, V+13.5 mm; third site: AP+9.0 mm, L+2.5 mm, V+12.0 mm; fourth site: AP+9.0 mm, L+3.5 mm, V+13.0 mm; fifth site: AP+10.5 mm, L+2.25 mm, V+12.0 mm; and sixth site: AP+10.5 mm, ML+3.25 mm, V+13.0 mm). In all cases, 6-OHDA solution was freshly prepared and stored on ice just before use. Each injection of 6-OHDA was made at a rate of 0.5 µl/min using a glass capillary (Nano injector 2000, WPI, Berlin, Germany), which was left in place for a further 4 min after each injection had been made. Following surgery, the monkeys were provided analgesia (as above) and kept in a warm incubator until they were well enough to be returned to their home cages. Postoperatively, the animals were treated with analgesics and antibiotics as described above. Three weeks after 6-OHDA lesion induction 20 µg of either CDNF (n = 4 animals) or GDNF (n = 4 animals) (PeproTech, London, UK) (two injections of 10 µg/3 µl of one of neurotrophic factor, dissolved in PBS) was intracerebrally injected (as described above for 6-OHDA injections) at two sites at the center of the lesion using the following coordinates: first site: AP+8.25 mm, L+3.0 mm, V+13.0 mm; second site: AP+9.75 mm, L+3.0 mm, V+12.5 mm. In a previous pilot trial we tested different experimental settings and SPECT acquisition time points. Based on individual SPECT scans we assume that recovery of DAT activity to normal levels is unlikely to occur in PBS treated animals. Therefore, we omitted this group in the treatment study, except of a single PBS-treated animal (S4 Fig), and focused on the comparison with the potent compound GDNF.

Physical and neurological examination

Clinical examinations included general condition [body weight, food consumption and excretion (faeces), exsiccosis, skin condition, attention] and neurological status (sensory limb reflex, handedness, movement activity pupillary reflex, eye tracking, orbicularis oculi reflex, gait, and tremor). In addition, animals were observed in their home cages to assess their behavior (attention, movement activity, and gait). Animals were examined in average twice weekly and at least for three days in a row after each surgical intervention. For the treatment study, examinations were discontinued for one week after every imaging session (SPECT, MRI). In the treatment study body weights were not included for evaluation due to possible impact of repeated anaesthetic procedures (animals were fasted prior to anaesthesia).

SPECT imaging

SPECT imaging was performed as previously described [49]. Briefly, a three-headed gamma camera (Prism 3000XP, Picker International, Cleveland, OH, USA) was upgraded with a dedicated small-animal imaging module (HiSPECT, Scivis, Göttingen, Germany). Each collimator head was equipped with a pyramidal collimator and multi-pinhole aperture plate (six pinholes). The inner diameter of each pinhole was 2.5 mm, which yielded a tomographic resolution of 2.1 mm and an average of axis sensitivity of 960 cps/MBq. The field of view (FoV) was 143 cm³. Images were acquired at 256 x 256 projection matrices with a pixel size of 1.78 mm over 10 gantry steps (30 projection angles) in a step-and-shoot mode. Up to four energy windows were acquired. An acquisition time of 300 s per gantry step and total scan time of 50.2 min was chosen. The photo peak energy was set to 159 keV with a window of $\pm 10\%$. Multi-energy window scatter correction was applied. The anesthetized animals were placed in a custom-made holder in a prone position and the head was fixed with ear bars. Image acquisition was initiated after reaching equilibrium state 2 h after injection of 50–60 MBq ¹²³I-FP-CIT (0.6–0.8 ml) (Datscan, Amersham Buchler, Braunschweig, Germany). SPECT reconstruction was performed using a dedicated iterative ordered subset expectation maximization (OSEM) algorithm consisting of three iterations and four subsets per iteration (HiSPECT). The reconstructed voxel size was 0.6 mm³. For quantification, brain activity was determined with HiSPECT software. Rectangular-shaped regions of interest (ROIs) of 991.4 mm³ volume were chosen manually for the left (STl) and right striatum (STr) and cerebellum (CB, 370.3 mm³) using corresponding magnetic resonance imaging (MRI, see below). Specific binding in the ST was calculated by subtracting the mean activity in the CB from the mean activity in the ST and dividing the result by the mean activity in the CB, i.e. (ST-CB)/CB. The binding ratio of the contralateral site served as an internal control and was set to 100%. For longitudinal monitoring of DAT activity a total of three scans per animals were performed (Fig 1).

Magnetic resonance imaging

For providing a reference of local brain anatomy, MRI was performed on a 3T clinical MR system (Magnetom TIM TRIO, Siemens Healthcare, Erlangen, Germany) [51]. Marmosets were scanned in supine position in the wrist coil under general anesthesia with diazepam (0.3 mg/kg i.m.), alfaxolon (10 mg/kg i.m., Alfaxan, Vetoquinol, UK), and glycopyrronium bromide (0.01 mg per animal i.m., Robinul, Riemser, Germany). The total measurement time for structural MRI at 0.4 mm isotropic resolution was about 10 min, thus eliminating the need to intubate the animal.

The three-dimensional (3D) imaging volume covered the head and upper chest with the read-out direction along the body axis. The FoV in the right-left and ventral-dorsal directions was 51.2 mm. T1-weighted (T1-w) contrast was achieved by magnetization-prepared rapid

acquisition of gradient echoes (MP-RAGE) using parameters recommended for humans (inversion time $TI = 0.9$ s, flip angle $\alpha = 9^\circ$, bandwidth $BW = 200$ Hz/pixel, echo time $TE = 4.06$ ms, repetition time $TR = 2.25$ s) [52]. The matrix of $320 \times 128 \times 128$ was acquired in 4:18 min. T2-w contrast was achieved by a 3D turbo spin echo (TSE) sequence with variable refocusing angle to preclude unexpected brain lesions. The matrix of $256 \times 128 \times 128$ was acquired in 5:26 min.

Post-processing of imaging data

The 2D digital imaging and communications in medicine (DICOM) MRI images in axial-to-coronal orientation were converted to 3D neuroimaging informatics technology initiative (NIFTI) volumes, changing from the radiological right-left convention to the left-right convention of the SPECT images. The T1-w volume was aligned to a custom-made T1-w template of the marmoset head and interpolated to 0.25 mm resolution to achieve consistent angulation of the horizontal plane. This was defined by the intercommissural line, as featured in the stereotaxic atlas of the National Institute of Neuroscience, Japan [53]. This T1-w volume then served as an individual anatomical reference to align the T2-w and SPECT volumes, using the FMRIB software library (FSL 4.1, Centre for Functional Magnetic Resonance Imaging of the Brain, University of Oxford, UK, www.fmrib.ox.ac.uk/fsl). For spatial alignment, the FSL linear registration tool (FLIRT), was used to determine the 3D rigid body transform (six parameters) by a mutual information criterion.

Cloning of marmoset CDNF cDNA and sequence analysis

Total RNA from the hippocampus was isolated using Tri-reagent (Thermo Fisher Scientific, Helsinki, Finland) following the manufacturer's instructions. First-strand cDNAs were synthesized with Revertaid Premium reverse transcriptase (Thermo Fischer Scientific) according to the manufacturer's instructions, using oligo(dT) primed total RNA (1 μ g) as a template. The following PCR primers containing either *Bam*HI or *Hind*III restriction sites were used: cj-CDNF_ *Hind*III_F (5' - ctctaagcttATGTGGTGC GCGAGCCCAGC -3') and cj-CDNF_ *Bam*HI_stop_R (5' - ataaggatccTCAGAGCTCTGCTTTGGGGTGTG -3') or cj-CDNF_ *Bam*HI_nostop_R (5' - ataaggatccGAGCTCTGCTTTGGGGTGTG -3'). PCR reactions were performed using the Phusion Hot Start II High-Fidelity DNA polymerase (Thermo Fisher Scientific). PCR products were restricted with *Bam*HI and *Hind*III and were cloned into *Bam*HI and *Hind*III sites in pCR3.1 vector (Invitrogen, Carlsbad, USA) and sequenced.

Alignment of amino acid sequences was performed with CLUSTAL O (version 1.2.0) software. Signal peptide cleavage sites were predicted using the SignalP 4.1 server (<http://www.cbs.dtu.dk/services/SignalP/>). Amino acid identity (%) of CDNF proteins was calculated by EMBOSS Needle program http://www.ebi.ac.uk/Tools/psa/emboss_needle/.

Histology

At the end of the experiments, animals were sacrificed for further histological evaluation. Animals underwent deep anaesthesia using a cocktail of ketamine, xylazine, and atropine. Subsequently, animals were transcardially perfused with 0.9% NaCl and 4% paraformaldehyde in PBS, pH 7.2. After storage of the heads in the fixative for 24 h at 4°C the brains were carefully removed, post-fixed in 4% paraformaldehyde in phosphate buffered saline and stored at 4°C until analysis. For the chronic CDNF infusion experiments, 3-mm-thick coronal brain slices were embedded in paraffin and cut into 3- μ m-thick sections. Hematoxylin and eosin (HE) staining was performed for standard microscopic pathology evaluation of relevant brain

structures (four slices of forebrain including midbrain, and two slices of hindbrain including cerebellum). As no abnormalities were observed in remote brain areas, we limited immunohistochemical evaluation on the coronal plane in the vicinity of the infusion site. For immunohistochemistry tissue sections were treated with citrate buffer (10 mM sodium citrate, pH 6). Immunohistochemistry was performed to assess inflammation using antibodies against CD3⁺ T-cells (1:50, A452, Dako, Hamburg, Germany), CD 20⁺ B-cells (1:200, M755, Dako) and MAC⁺ macrophages/ activated microglia (1:300, M0747, Dako). Discovery universal secondary antibody (760–4205, Discovery universal secondary antibody, Roche, Basel, Switzerland) was used. Antibodies were visualized using DAB detection kit (760–124, DABMap, Roche, Basel, Switzerland). Slides were counterstained using Mayer's hemalaun solution. Control sections were incubated in absence of primary antibody. Lymph nodes of healthy marmosets served as positive control for inflammatory markers. The degree of inflammation within the injected brain hemisphere was assessed on representative on HE-stained and CD3-stained coronal sections using a semiquantitative score (- no, + mild, ++ moderate, +++ severe). Regions of interest were the vicinity of cannula track (a region of approx. 50 μ m around the cannula track, referred as "infiltrates in the vicinity of cannula track") and a broad area (including striatum, corpus callosum and cerebral cortex, referred as "widespread perivascular infiltrates").

For the treatment study, post-fixed brains were stored in 30% sucrose, frozen and cut into 40- μ m-thick sections. Antibodies against CDNF (1:1000, #4343, ProSci, Poway, CA, USA), tyrosine hydroxylase (1:500, Biotrend, Cologne, Germany) and dopamine transporters (1:1000, D6944, Sigma-Aldrich) were used overnight. Appropriate secondary antibodies were used (1:200, Vector Laboratories, Axxora Deutschland GmbH, Lörrach, Germany). Sections were treated with avidin-biotin-peroxidase complex (PK-6100, Vectastain Elite ABC, Vector Laboratories). DAB was used as the chromogen (Vector Laboratories). Control sections were incubated in absence of primary antibody. Digital images of immunostained tissue sections were acquired using an Axiophot II microscope (Zeiss, Germany). Distribution of CDNF after chronic delivery was assessed on CDNF-ir representative coronal sections using a semiquantitative score (- no signal, + low, ++ moderate, +++ high).

Numbers of TH-immunoreactive (TH-ir) neurons in the caudate nucleus were assessed on coronal TH-stained sections. 10–12 representative sections at interval of 30 μ m were used to cover the rostro-caudal extension of the striatum of each animal. Counting of TH-immunoreactive cells was performed with an Axioplan II light microscope (Zeiss) using a counting grid on 10-fold magnification placed on all caudate areas of the section. Only cells positive for TH that possessed a clear and vital neuronal morphology were included for counting. The number of positive cells per cm² was reported. Numbers of TH-ir neurons in the *substantia nigra pars compacta* (SNc) were assessed on coronal TH-stained 30 μ m thick sections. Every 8th section was used to cover the rostral-caudal extension of the SNc. Counting of TH-ir neurons was performed as described above.

Statistical analysis

Data are presented as mean \pm standard deviation (SD). Data were analyzed using GraphPad Prism (version 5.00 for Windows, GraphPad Software, San Diego, CA, USA) and SigmaPlot 11 (Systat Software Inc., San Jose, CA, USA). Statistical analyses of the SPECT study included repeated measures analysis of variance (ANOVA) followed by post hoc Holm-Sidak test and Bonferroni-Holm correction for adjusted p values. Unpaired Student's t-tests were performed for quantitative histological analysis. Differences were considered statistically different if $p < 0.05$. Data analysis was performed in a blind fashion.

Results

Histopathological changes after high chronic CDNF infusion

The tolerability of CDNF was tested starting with low concentrations of the growth factor protein. Because no pathological effects were detected after a single intracerebral injection of 30 μg CDNF in previous experiments (S1 Fig), higher doses of CDNF were delivered chronically for 4 weeks using osmotic pumps. Histopathologically, no abnormalities were detected in the marmoset receiving 10 μg CDNF per day (with a total amount of 280 μg CDNF over a 4-week period of delivery) and the vehicle control. Therefore, we focussed on higher doses in the actual experiments.

Four marmosets received a chronic CDNF infusion of 15 $\mu\text{g}/\text{day}$ for 28 days (420 μg CDNF in total). In two animals (Fig 2, animals # 13685 and # 13565), no obvious histopathological abnormalities were observed. In a single animal histopathological analysis revealed a strong parenchymal and perivascular reaction composed of CD3⁺ and CD20⁺ infiltrates in the absence of macrophages or activated microglia (Fig 2, animal # 13864). A fourth animal (animal # 12887) showed a local, moderate inflammation restricted to perivascular areas in the vicinity of cannula track. These results indicate potential immunogenicity of CDNF in single animals when administered in high doses. However, semiquantitative analysis of CDNF-ir tissue distribution, revealed that CDNF-ir was completely absent in a single high-dose CDNF animal (S2 Fig, Table 1, animal # 13685) and this might explain the absence of histopathology in this particular animal. Moreover, the distribution pattern of infiltrates observed in animal # 12887 is partly matching with CDNF-ir distribution. However, we cannot rule out the possibility that injected CDNF had become contaminated and caused the observed histopathology in two of four animals. Besides the mentioned histopathology, the general condition of the animals was not affected. Body weights remained stable (S3 Fig) and the animals showed no abnormal behavior. The CDNF dose used in the neurorestorative treatment approach was about 15 times less than the maximum tolerated dose.

CDNF increases striatal DAT activity after mild 6-OHDA lesions

To maintain the regenerative capacity of the brain a mild 6-OHDA lesion protocol was established. Injections of 6-OHDA were targeted to the caudate nucleus leading to a notable but mild reduction of dopamine transporter activity (Fig 3). 6-OHDA lesions did not lead to overt behavioral impairment or loss of substantia nigra neurons (S1 Table). In some cases, transient and inconsistent tremor was observed within the first 2 weeks after lesioning.

Quantitative SPECT analysis of the affected brain area confirmed a moderate reduction of striatal DAT binding with values of $65.91 \pm 6.47\%$ in the CDNF group and $79.31 \pm 3.69\%$ in the GDNF group, compared with their corresponding contralateral untreated sides (Fig 3B and 3C). Three weeks after inducing lesions, the animals received intracerebral injections of the neurotrophic factors. In CDNF-treated animals, we observed a significant ($*p = 0.023$, [$F_{2,11} = 33.32$, $p < 0.001$]) recovery of striatal DAT binding of approximately 10% up to $76.32 \pm 1.38\%$ 8 weeks after treatment. By contrast, in the GDNF-treated group, DAT binding only slightly increased, on average to $82.20 \pm 6.31\%$. Two animals in the GDNF-treated group responded to the treatment (approximately 7% recovery). Two other animals did not show any obvious change in DAT binding after GDNF treatment. In summary, no statistical differences were observed in the GDNF group. As a control a single animal was treated with PBS after 6-OHDA lesion paradigm. No spontaneous recovery was observed in DAT imaging (see S4 Fig).

At the end of the experiment, a histological examination was performed (Fig 4). The topography and intensity of TH and DAT immunoreactivity of the lesioned caudate nucleus

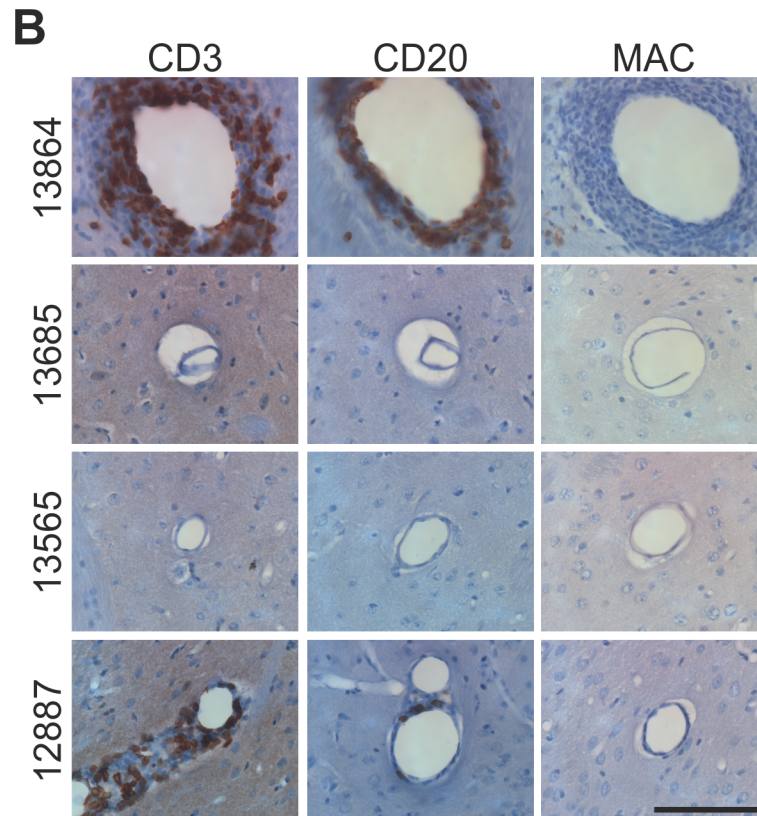


Fig 2. Histopathological assessment of the caudate nucleus of chronically CDNF-infused animals (CDNF: 15µg/day for 28 days; totally 420 µg). Perivascular infiltrates positive for CD3 and CD20 were observed in two animals (animals # 13864 and # 12887) out of four analysed. MAC-positive macrophages/activated microglia were absent. Scale bar = 100µm.

doi:10.1371/journal.pone.0149776.g002

corresponded to the picture observed in SPECT. However, detailed analysis revealed structural changes on a microscopic level within the lesioned caudate nucleus of GDNF-treated animals. High numbers of TH-positive cells were observed within the lesioned area, and many of them could be clearly assigned to vital neurons because they possessed a typical branching pattern (Fig 5B and 5C). Furthermore, a high fraction of small TH-positive structures (Fig 5D) and TH-positive varicosities (Fig 5E) were observed within the GDNF-treated lesioned caudate.

Table 1. Tolerability of chronic CDNF delivery: concentrations of CDNF in comparison to the degree of histopathology and CDNF-ir tissue distribution. Histopathological scoring was based on HE-staining and CD3 immunohistochemistry (- no, + mild, ++ moderate, +++ severe). CDNF-ir distribution (See also S2 Fig) was semi quantitatively assessed on coronal sections (- no signal, + low, ++ moderate, +++ high).

Animal ID	Treatment	Histopathology		
		Infiltrates in the vicinity of cannula track	Widespread perivascular infiltrates	CDNF-ir distribution
13864	15µg CDNF	+++	+++	+++
13685	15µg CDNF	+	-	-
13565	15µg CDNF	-	-	+++
12887	15µg CDNF	++	+	++
13601	10µg CDNF	-	-	+
13639	PBS	-	-	-

doi:10.1371/journal.pone.0149776.t001

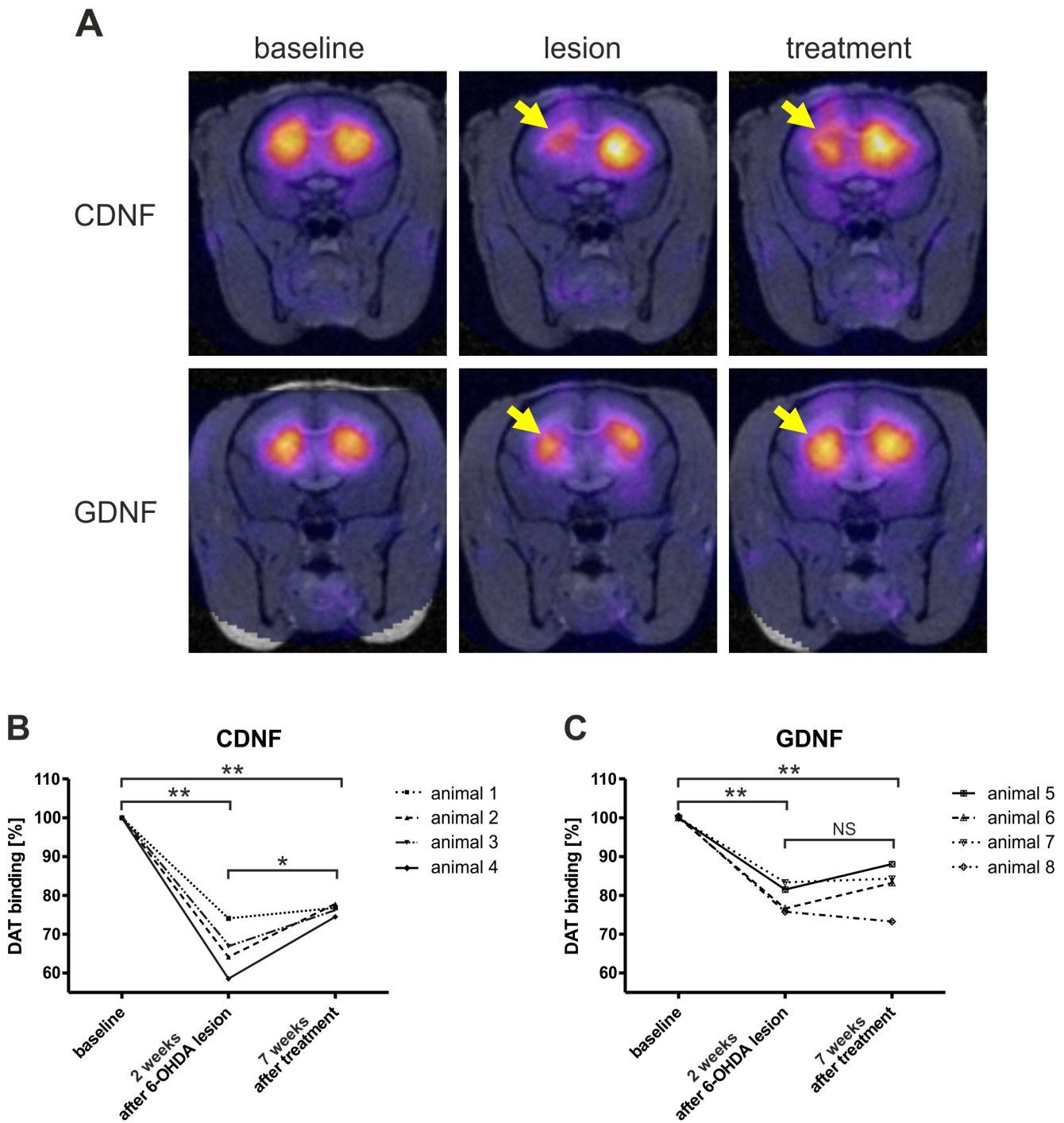


Fig 3. (A) Representative ^{123}I -FP-CIT SPECT images of CDNF (upper row) and GDNF treated (lower row) marmosets. Reduced DAT-binding was observed after mild 6-OHDA lesions when targeted to the caudate nucleus (middle row, indicated by arrows). Treatment via intracerebral injection of either 20 μg of CDNF (upper row) or 20 μg of GDNF (lower row), lead to obvious recovery on the level of DAT integrity (indicated by arrows). (B, C) Treatment effects were evaluated by quantitative analysis of ^{123}I -FP-CIT SPECT. Animals showed a significant increase of DAT-binding ($*p = 0.023$, $[F_{2,11} = 33.32, p < 0.001]$) when treated with CDNF (B). In the GDNF group single animals responded to the treatment with GDNF (C, animals #5 and #6). However, no significant recovery was observed in the GDNF-treated group. $*p < 0.05$, $**p < 0.01$, NS = not significant.

doi:10.1371/journal.pone.0149776.g003

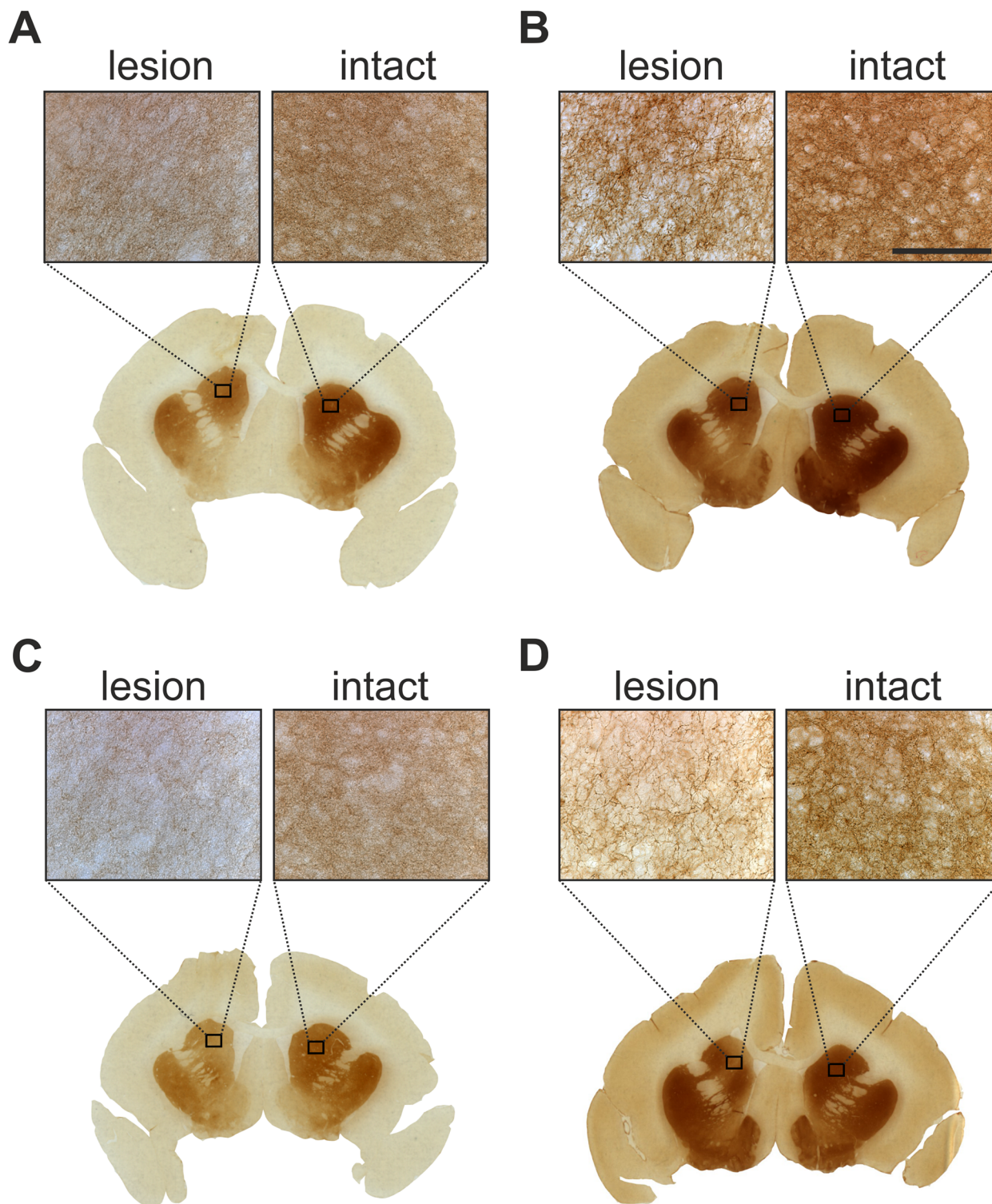


Fig 4. Immunohistochemistry of the caudate nucleus was performed at the end of experiment. Sections were stained for DAT (A / C) and TH (B / D). The affected brain areas showed moderate dopaminergic integrity after treatment with CDNF (A / B) and GDNF (C / D). Scale bar: 100 μ m.

doi:10.1371/journal.pone.0149776.g004

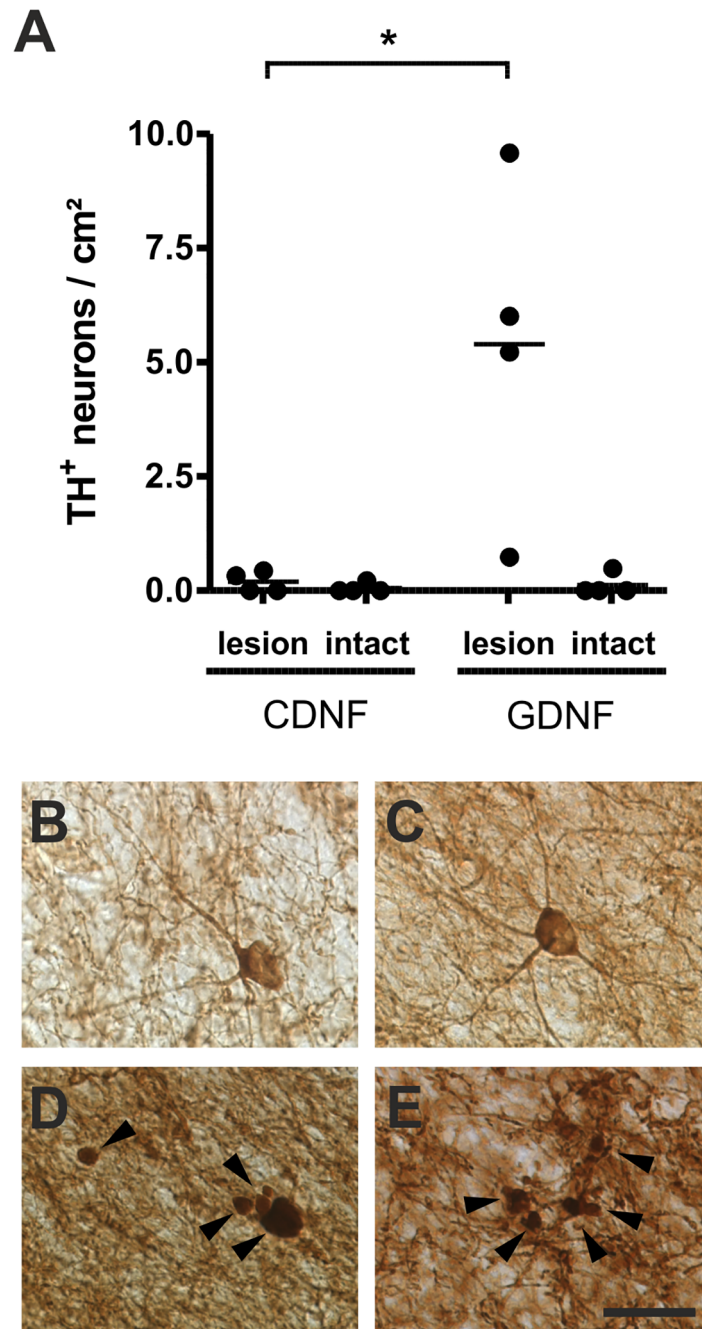


Fig 5. Structural effects of GDNF treatment on TH-immunoreactivity was observed within the lesioned caudate nucleus (B–E). TH-positive neurons showed a typical branching pattern (B/C). The number of TH-positive neurons was significantly increased in the GDNF treated lesioned caudate nucleus (A) compared to CDNF treated animals ($p < 0.05$). Moreover, a high fraction of small TH-positive structures (D) and TH-positive varicosities (E) were observed within the GDNF-treated lesioned caudate. Mean. $*p < 0.05$. Scale bar, 25 μ m.

doi:10.1371/journal.pone.0149776.g005

Interestingly, no structural changes were observed in TH-stained sections of CDNF treated animals. Moreover, no obvious changes were observed in DAT immunoreactivity in any of the experimental groups.

Quantification revealed increased numbers of TH-positive neurons in the lesioned GDNF-treated caudate nucleus (Fig 5A, 5.39 ± 3.64 cells/cm²). This effect was significant (* $p < 0.05$, unpaired Student's t-test) when compared with the lesioned CDNF-treated caudate nucleus (0.19 ± 0.23 cells/cm²). As expected, TH-positive neuronal counts were negligible in the contralateral site of marmosets from the GDNF- (0.12 ± 0.24 cells/cm²) and CDNF-treated groups (0.05 ± 0.11 cells/cm²). Quantification of TH-ir in midbrain showed no statistical difference between lesioned and contralateral SNc and treatment groups, respectively (S1 Table).

Amino acid sequence of marmoset CDNF

To verify the *Callithrix jacchus* CDNF sequence we cloned a corresponding cDNA from the hippocampal tissue of a female marmoset. The obtained nucleotide sequence was identical to the coding sequence of GenBank GAMQ01005170 mRNA (translation JAB36681.1). Alignment of CDNF amino acid sequences from marmoset, human [1], chimpanzee (*Pan troglodytes*; GenBank prediction XP_507666.2) and rhesus macaque (*Macaca mulatta*; GenBank prediction NP_001180755.1) is presented in Fig 6. The identity of mature human CDNF to marmoset, macaque, and chimpanzee sequences is 93.8%, 100%, and 99.4%, respectively (Table 2). Closely resembling human CDNF and the predicted CDNF sequences of chimpanzee and macaque, marmoset CDNF consists of 187 amino acid (aa) residues with a predicted signal peptide of 26 aa, thus resulting in a mature protein of 161 aa, with eight evolutionarily conserved cysteine residues with identical spacing determining the protein fold [1, 7]. A N-linked glycosylation site of human CDNF at position 57N [13] is lacking from the marmoset CDNF, whereas it is conserved in chimpanzee and rhesus macaque, which, differently from marmoset, belong to apes and Old World monkeys, respectively. However, the O-linked glycosylation site at position 181T of human CDNF [54] is conserved in all primate sequences aligned. A putative ER-retention signal KTEL is present at the C-terminal end of human CDNF [55–56] and in the CDNF sequence of chimpanzees and rhesus macaques, whereas in marmoset CDNF, the signal is KAEL where the polar threonine (T) is replaced with a neutral alanine (A) residue.

Discussion

Tolerability of CDNF

The present CDNF chronic infusion study is a first approach in nonhuman primates to define controlled conditions for a safe application for CDNF protein in future therapies.

High-dose chronic infusion of CDNF (15 µg/day for 28 days) led to histopathological changes in two out of four animals. The composition of perivascular infiltrates observed indicated an immunogenicity of recombinant human CDNF in the marmoset brain, presumably caused by interspecies differences. It is also possible that the CDNF protein preparation contained minor impurities inducing the immunological reaction observed. Moreover, we reported inconsistent drug delivery in at least one case. However, the degree of histopathological changes largely matched with the distribution of CDNF-ir, indicating a dose dependency of CDNF immunogenicity. The use of more reliable delivery techniques such as convection-enhanced delivery should be considered for future applications [34–36]. The animal that received a daily concentration of 10 µg CDNF did not show any abnormalities. Although this result is not representative, it is in line with results in rats with a 4–5 times smaller brain where infusion of CDNF at 4.5 µg/day for 2 weeks did not induce histopathological changes [3].

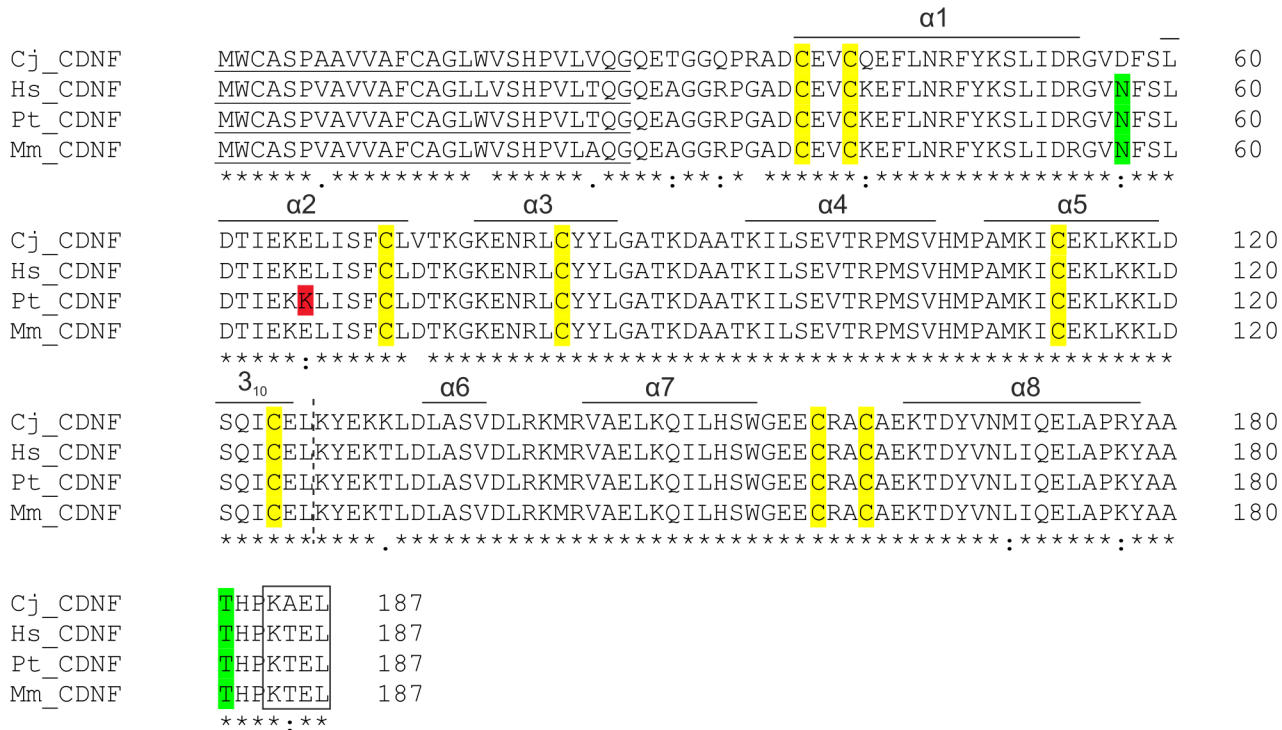


Fig 6. Alignment of marmoset (Cj), human (Hs), chimpanzee (Pt), and macaque (Mm) CDNF amino acid sequences by CLUSTAL O (version 1.2.0) software. Identical amino acids are marked with an asterisk, physicochemically highly similar with a colon, and similar with a dot. Predicted signal sequences (SignalP 4.1 Server <http://www.cbs.dtu.dk/services/SignalP/>) of marmoset, chimpanzee and macaque CDNF (residues 1–26; underlined) are equal in length to the verified signal peptide of human CDNF [1]. Eight conserved cysteine residues with identical spacing of the mature CDNF are indicated in yellow. N-linked glycosylation site of human CDNF at position 57N [13] and O-linked glycosylation site at position 181T [52] is indicated in green. The C-terminal ER-retention motif KAEI/KTEL is boxed. Alpha-helical regions of CDNF are indicated above the sequences according to [7] (helices α1–α5 and turn of 3₁₀ helix) and [9] (helices α6–α8). The division between N-terminal saposin-like domain and C-terminal SAP-domain is indicated by a vertical dashed line.

doi:10.1371/journal.pone.0149776.g006

The tolerability of GDNF in marmosets was not investigated in the present study. However, therapeutic doses of GDNF are well tolerated in Parkinsonian marmosets [22, 57]. By contrast, clinical symptoms and histopathological changes can appear after intraputamin and intraventricular chronic infusion of high doses of GDNF in Old World monkeys [20, 42, 58–59] and PD patients [59]. In particular, meningeal thickening and cerebellar lesions can appear after long-term infusion of high doses of GDNF [42]. Whether CDNF can cause such symptoms (using comparable study parameters) is unclear and warrants further investigation.

Despite the histopathology observed at high and chronic doses, we do recommend CDNF for therapeutic use in marmosets because CDNF is well tolerated in lower concentrations. In the presented treatment approach, the concentration used was more than 20 times less that used in the chronic infusion protocol in which pathological changes occurred. Observations in

Table 2. Amino acid identity (%) of CDNF proteins between human and selected nonhuman primates calculated by EMBOSS Needle software. Signal peptide sequences have been omitted.

	<i>Homo sapiens</i>	<i>Pan troglodytes</i>	<i>Macaca mulatta</i>	<i>Callithrix jacchus</i>
<i>Homo sapiens</i>	100	99.4	100	93.8
<i>Pan troglodytes</i>		100	99.4	93.2
<i>Macaca mulatta</i>			100	93.8
<i>Callithrix jacchus</i>				100

doi:10.1371/journal.pone.0149776.t002

rodents also confirm that CDFN is well tolerated, even at high therapeutic doses [1, 3]. However, further preclinical studies are needed with CDFN of good-manufacturing-practice (GMP) quality to determine the biosafety of CDFN.

Neuroregeneration of CDFN and GDNF in the mild 6-OHDA lesion model

In the presented study, we used 6-OHDA to induce moderate to mild caudate lesions in common marmosets, resulting in transient or absent motor dysfunction. However, the impact of the lesion on dopaminergic striatal areas was sufficiently strong to be clearly detected and quantified by ^{123}I -FP-CIT SPECT. The SPECT method employed has been previously validated in various studies, and clearly correlated with dopamine dysfunction in models of PD [5, 49, 60–63]. Moreover, this method has gained increasing clinical importance in PD diagnostics [64–65].

In the neurorestorative approach, a significant but moderate increase of DAT binding was observed after treatment with CDFN. Recovery was less prominent than that seen in rodent studies [1–3] and might be explained by the limited regenerative capacity and the larger dimensions of the primate brain compared with rodents. Alternatively, CDFN may work better with a larger lesion and have modest effects with smaller lesions, because it has no effects to the striatum of unlesioned rodent brains [3–4]. From the SPECT data, we cannot distinguish between functional and structural restoration of the dopaminergic innervation. However, previous studies showed a robust correlation of SPECT and TH-ir within the affected areas [60–63]. In comparison with the criterion standard GDNF, CDFN treatment was more effective. This can be explained by the limited diffusion of GDNF compared to CDFN [3, 41] and dose response [3]. More importantly, the differences in the structure and mode of action between CDFN and GDNF may explain the outcome (delayed response of GDNF, long lasting effects of CDFN) [1]. It should be noted that CDFN is structurally unrelated to the classical neurotrophic factors [8] and can rescue neurons when injected into the cell cytoplasm [9]; however, its receptor and signaling pathways remain unclear.

Individual animals responded slightly to GDNF treatment via increased DAT activity, but the effect was statistically not significant. However, at the microscopic level, we found obvious structural effects on TH-ir neurons after treatment with GDNF, but not in marmosets from the CDFN-treated group. The discrepancies between low response in DAT binding and the strong appearance of TH-ir neurons after GDNF treatment are difficult to address. As discussed above, inconsistent drug delivery may account for the low response in the GDNF treatment group [34–36]. Nevertheless, the low impact on DAT activity cannot be explained by insufficient GDNF dose, since the impact of GDNF on TH-ir was very strong. Moreover, we delivered the trophic factors into two injection sites and by that we provided a better distribution of the factors and reduced the risk of insufficient drug delivery. Since only the endpoint of experiment was accessible for histological analysis, only obvious histological changes as mentioned above, may be considered for interpretation. GDNF rather strongly upregulates TH expression and that is one obvious explanation [19]. Possibly, TH-ir striatal neurons do not contribute to DAT activity in a sufficiently strong manner to be detected with SPECT. This possibility is supported by the fact that DAT-ir appeared normal in contrast to TH in the GDNF-treated caudate nucleus. Speculatively, an increase in TH-ir in striatal neurons may compensate for the indistinct dopamine transporter integrity. Whether local interneurons adopted a TH-ir phenotype or whether these cells were newly created remains unclear. Interestingly, striatal dopaminergic neurons were found in PD patients treated with L-DOPA (but not with GDNF), but unlike in the presented study in which marmosets were immunoreactive for TH only, striatal neurons in

human PD samples were DAT-ir [66]. This may be explained by differences between humans in non-human primates. Alternatively, striatal TH-ir neurons emerged from effects that were genuine to GDNF-treatment. However, an increase of TH-ir cells is reported in the literature in the context of regeneration and GDNF in Parkinsonian rhesus monkeys [67]. Therefore, we can assume a certain neurorestorative potential also for GDNF, although in a rather limited fashion. By contrast with GDNF, an effect of CDFN on the TH-ir striatal neuron population was not detected in these mildly lesioned animals. Our data support the idea that CDFN and GDNF have different mechanisms of action.

The choice of animal model and treatment approach is essential for testing new therapeutic agents for PD. Neurotrophic factors are strongly neuroprotective, but some of them, such as GDNF, NRTN, CDFN and MANF have also neurorestorative activities [1, 3, 68]. GDNF has shown prominent neurorestorative effects in the primate brain [22, 41]. However, because neurotrophic factor therapies are actually applied to patients at a late stage of disease [37], the presented study focussed on neurorestoration. The 6-OHDA model is considered to induce a robust pathology on DA neurons [49, 69] in which functional regeneration and full anatomical restoration normally does not occur apart from a few exceptions [70–71]. Therefore, the 6-OHDA model is a very good model as it does not mask the effect of the test compound. By contrast, the strong chronicity of the neurotoxin may deplete the endogenous regenerative potential of the brain, and thus prevent the putative beneficial effects of test compounds. In our approach DA neurons in SNc seem not to be affected by the mild impact of striatal lesion as histology performed at the end of experiment may suggest. Taking this into account, the presented mild 6-OHDA lesion protocol effects robust striatal DA neuron pathology, at least on the level of DAT imaging, while maintaining the endogenous regenerative capacity of the brain (in particular the SN), and thus enabling evaluation of the compounds tested. However, since the PBS control group is missing, further investigation is needed to support the suitability and reliability of the proposed lesion paradigm.

In contrast to the viral vector delivered α -syn model of PD, 6-OHDA pathology is restricted to the dopaminergic system. Therefore, it would be interesting to test CDFN in the α -syn model in marmosets [72–74], especially, since GDNF showed no neuroprotective effects in the rat α -syn model [25–26].

Comparison of marmoset CDFN amino acid sequence within primates

The amino acid sequence of the predicted mature marmoset CDFN is 93.8% identical to that of human CDFN and contains eight cysteine residues of conserved spacing. The predicted CDFN amino acid sequence of our closest living relatives, the chimpanzee, and the rhesus macaque, are even more closely related to the mature human CDFN with an amino acid identity of 99.4% and 100%, respectively. Because of these close homologies, recombinant human CDFN presumably has neuroprotective activities not only in marmosets, but potentially in other non-human primates.

Recent publications suggest that human MANF is retained in the ER by the C-terminal RTDL sequence via interaction with Lys-Asp-Glu-Leu (KDEL) endoplasmic reticulum protein retention receptor [75–76]. Whether the C-terminal KTEL sequence in human, chimpanzee, and rhesus macaque or the KAEL sequence in the marmoset CDFN has a similar role remains unclear. Interestingly, an N-linked glycosylation site of human CDFN sequence [13] is also present in the predicted amino acid sequence of the chimpanzee and rhesus monkey, whereas in the sequence of marmoset CDFN, the site is missing. Although glycosylation is not required for the secretion of CDFN [1, 54], the site for N-linked glycosylation may serve some other regulatory function in close human relatives.

Conclusion

The study demonstrated a beneficial effect of CDFN on DAT activity in a mild 6-OHDA-mediated model of PD in marmoset monkeys. In comparison with CDFN, GDNF treatment was less effective at the level of DAT imaging. However, increased numbers of TH-ir neurons were observed within the lesioned caudate nucleus, indicating the strong regenerative potential of GDNF. In marmosets, intracerebral CDFN treatment was safe when applied at low dose. Chronic delivery of CDFN at a concentration of 15 μ g/day for 28 days lead to histopathological effects.

Supporting Information

S1 Fig. Photographs of the striatum 60 days after single intracerebral injection of 30 μ g CDFN. Histological evaluation was based on HE-staining. No pathological abnormalities were observed, with the exception of mild edema at the tip of the needle track (inset, indicated by arrows). Scale bars: overview = 1 mm, inset = 200 μ m.

(TIF)

S2 Fig. Coronal sections of CDFN-stained marmoset brains after high dose chronic infusion of 15 μ g CDFN (upper row), 10 μ g CDFN (lower right) and PBS (lower left). CDFN-ir distribution was restricted to striatal areas, the vicinity of cannula track or absent (target areas indicated by black arrows).

(TIF)

S3 Fig. Chronic infusion of CDFN: Body weights remained stable with only transient fluctuations within a range of less than 10%.

(TIF)

S4 Fig. Quantitative analysis of 123I-FP-CIT SPECT. No spontaneous recovery of DAT activity was observed in the PBS-treated control animal.

(TIF)

S1 Table. Density of TH-ir neurons in the substantia nigra pars compacta (SNc). No significant changes were observed between ipsilateral and contralateral SNc of 6-OHDA-lesioned animals after treatment with neurotrophic factors. Moreover, no significant changes were detected between treatment groups. Data are given as mean \pm SD.

(DOCX)

Acknowledgments

The authors wish to thank S. Leineweber, O. Rautz, L.M. Krautheim and J. Wülker for expert animal care and K. Hoffmann, J. Schmiereck and J. Schell for technical support.

Author Contributions

Conceived and designed the experiments: EGR KK MS EF. Performed the experiments: EGR AE CS GH JK BM. Analyzed the data: EGR AE PL GH MS EF. Contributed reagents/materials/analysis tools: BM MS GH EF. Wrote the paper: EGR PL GH MS EF.

References

1. Lindholm P, Voutilainen MH, Lauren J, Peranen J, Leppanen VM, Andressoo JO, et al. Novel neurotrophic factor CDFN protects and rescues midbrain dopamine neurons in vivo. *Nature*. 2007; 448 (7149):73–7. Epub 2007/07/06. PMID: [17611540](#)

2. Voutilainen MH, Back S, Porsti E, Toppinen L, Lindgren L, Lindholm P, et al. Mesencephalic astrocyte-derived neurotrophic factor is neurorestorative in rat model of Parkinson's disease. *J Neurosci*. 2009; 29(30):9651–9. Epub 2009/07/31. doi: [10.1523/JNEUROSCI.0833-09.2009](https://doi.org/10.1523/JNEUROSCI.0833-09.2009) PMID: [19641128](https://pubmed.ncbi.nlm.nih.gov/19641128/)
3. Voutilainen MH, Back S, Peranen J, Lindholm P, Raasmaja A, Mannisto PT, et al. Chronic infusion of CDNF prevents 6-OHDA-induced deficits in a rat model of Parkinson's disease. *Exp Neurol*. 2011; 228(1):99–108. Epub 2010/12/28. doi: [10.1016/j.expneurol.2010.12.013](https://doi.org/10.1016/j.expneurol.2010.12.013) PMID: [21185834](https://pubmed.ncbi.nlm.nih.gov/21185834/)
4. Airavaara M, Harvey BK, Voutilainen MH, Shen H, Chou J, Lindholm P, et al. CDNF protects the nigrostriatal dopamine system and promotes recovery after MPTP treatment in mice. *Cell Transplant*. 2012; 21(6):1213–23. Epub 2011/09/29. doi: [10.3727/096368911X600948](https://doi.org/10.3727/096368911X600948) PMID: [21943517](https://pubmed.ncbi.nlm.nih.gov/21943517/)
5. Bäck S, Peränen J, Galli E, Pulkila P, Lonka-Nevalaita L, Tamminen T, et al. Gene therapy with AAV2-CDNF provides functional benefits in a rat model of Parkinson's disease. *Brain Behav*. 2013; 3(2):75–88. Epub 2013/03/28. doi: [10.1002/brb3.117](https://doi.org/10.1002/brb3.117) PMID: [23532969](https://pubmed.ncbi.nlm.nih.gov/23532969/)
6. Ren X, Zhang T, Gong X, Hu G, Ding W, Wang X. AAV2-mediated striatum delivery of human CDNF prevents the deterioration of midbrain dopamine neurons in a 6-hydroxydopamine induced parkinsonian rat model. *Exp Neurol*. 2013; 248:148–56. Epub 2013/06/15. doi: [10.1016/j.expneurol.2013.06.002](https://doi.org/10.1016/j.expneurol.2013.06.002) PMID: [23764500](https://pubmed.ncbi.nlm.nih.gov/23764500/)
7. Parkash V, Lindholm P, Peranen J, Kalkkinen N, Oksanen E, Saarma M, et al. The structure of the conserved neurotrophic factors MANF and CDNF explains why they are bifunctional. *Protein Eng Des Sel*. 2009; 22(4):233–41. Epub 2009/03/05. doi: [10.1093/protein/gzn080](https://doi.org/10.1093/protein/gzn080) PMID: [19258449](https://pubmed.ncbi.nlm.nih.gov/19258449/)
8. Lindholm P, Saarma M. Novel CDNF/MANF family of neurotrophic factors. *Dev Neurobiol*. 2010; 70(5):360–71. Epub 2010/02/27. doi: [10.1002/dneu.20760](https://doi.org/10.1002/dneu.20760) PMID: [20186704](https://pubmed.ncbi.nlm.nih.gov/20186704/)
9. Hellman M, Arumae U, Yu LY, Lindholm P, Peranen J, Saarma M, et al. Mesencephalic astrocyte-derived neurotrophic factor (MANF) has a unique mechanism to rescue apoptotic neurons. *J Biol Chem*. 2011; 286(4):2675–80. Epub 2010/11/05. doi: [10.1074/jbc.M110.146738](https://doi.org/10.1074/jbc.M110.146738) PMID: [21047780](https://pubmed.ncbi.nlm.nih.gov/21047780/)
10. Lindahl M, Danilova T, Palm E, Lindholm P, Voikar V, Hakonen E, et al. MANF Is Indispensable for the Proliferation and Survival of Pancreatic beta Cells. *Cell Rep*. 2014; 7(2):366–75. Epub 2014/04/15. doi: [10.1016/j.celrep.2014.03.023](https://doi.org/10.1016/j.celrep.2014.03.023) PMID: [24726366](https://pubmed.ncbi.nlm.nih.gov/24726366/)
11. Palgi M, Lindstrom R, Peranen J, Piepponen TP, Saarma M, Heino TI. Evidence that DmMANF is an invertebrate neurotrophic factor supporting dopaminergic neurons. *Proc Natl Acad Sci U S A*. 2009; 106(7):2429–34. Epub 2009/01/24. doi: [10.1073/pnas.0810996106](https://doi.org/10.1073/pnas.0810996106) PMID: [19164766](https://pubmed.ncbi.nlm.nih.gov/19164766/)
12. Petrova P, Raibekas A, Pevsner J, Vigo N, Anafi M, Moore MK, et al. MANF: a new mesencephalic, astrocyte-derived neurotrophic factor with selectivity for dopaminergic neurons. *J Mol Neurosci*. 2003; 20(2):173–88. Epub 2003/06/10. PMID: [12794311](https://pubmed.ncbi.nlm.nih.gov/12794311/)
13. Apostolou A, Shen Y, Liang Y, Luo J, Fang S. Armet, a UPR-upregulated protein, inhibits cell proliferation and ER stress-induced cell death. *Exp Cell Res*. 2008; 314(13):2454–67. Epub 2008/06/20. doi: [10.1016/j.yexcr.2008.05.001](https://doi.org/10.1016/j.yexcr.2008.05.001) PMID: [18561914](https://pubmed.ncbi.nlm.nih.gov/18561914/)
14. Mizobuchi N, Hoseki J, Kubota H, Toyokuni S, Nozaki J, Naitoh M, et al. ARMET is a soluble ER protein induced by the unfolded protein response via ERSE-II element. *Cell Struct Funct*. 2007; 32(1):41–50. Epub 2007/05/18. PMID: [17507765](https://pubmed.ncbi.nlm.nih.gov/17507765/)
15. Tadimalla A, Belmont PJ, Thuerauf DJ, Glassy MS, Martindale JJ, Gude N, et al. Mesencephalic astrocyte-derived neurotrophic factor is an ischemia-inducible secreted endoplasmic reticulum stress response protein in the heart. *Circ Res*. 2008; 103(11):1249–58. Epub 2008/10/18. doi: [10.1161/CIRCRESAHA.108.180679](https://doi.org/10.1161/CIRCRESAHA.108.180679) PMID: [18927462](https://pubmed.ncbi.nlm.nih.gov/18927462/)
16. Hoffer BJ, Hoffman A, Bowenkamp K, Huettl P, Hudson J, Martin D, et al. Glial cell line-derived neurotrophic factor reverses toxin-induced injury to midbrain dopaminergic neurons in vivo. *Neurosci Lett*. 1994; 182(1):107–11. Epub 1994/11/21. PMID: [7891873](https://pubmed.ncbi.nlm.nih.gov/7891873/)
17. Kearns CM, Gash DM. GDNF protects nigral dopamine neurons against 6-hydroxydopamine in vivo. *Brain Res*. 1995; 672(1–2):104–11. Epub 1995/02/20. PMID: [7749731](https://pubmed.ncbi.nlm.nih.gov/7749731/)
18. Tomac A, Lindqvist E, Lin LF, Ogren SO, Young D, Hoffer BJ, et al. Protection and repair of the nigrostriatal dopaminergic system by GDNF in vivo. *Nature*. 1995; 373(6512):335–9. Epub 1995/01/26. PMID: [7830766](https://pubmed.ncbi.nlm.nih.gov/7830766/)
19. Gash DM, Zhang Z, Ovadia A, Cass WA, Yi A, Simmerman L, et al. Functional recovery in parkinsonian monkeys treated with GDNF. *Nature*. 1996; 380(6571):252–5. Epub 1996/03/21. PMID: [8637574](https://pubmed.ncbi.nlm.nih.gov/8637574/)
20. Zhang Z, Miyoshi Y, Lapchak PA, Collins F, Hilt D, Lebel C, et al. Dose response to intraventricular glial cell line-derived neurotrophic factor administration in parkinsonian monkeys. *J Pharmacol Exp Ther*. 1997; 282(3):1396–401. Epub 1997/10/08. PMID: [9316852](https://pubmed.ncbi.nlm.nih.gov/9316852/)
21. Kirik D, Georgievska B, Bjorklund A. Localized striatal delivery of GDNF as a treatment for Parkinson disease. *Nat Neurosci*. 2004; 7(2):105–10. Epub 2004/01/30. PMID: [14747832](https://pubmed.ncbi.nlm.nih.gov/14747832/)

22. Eslamboli A. Assessment of GDNF in primate models of Parkinson's disease: comparison with human studies. *Rev Neurosci*. 2005; 16(4):303–10. Epub 2006/03/08. PMID: [16519007](#)
23. Eberling JL, Kells AP, Pivrotto P, Beyer J, Bringas J, Federoff HJ, et al. Functional effects of AAV2-GDNF on the dopaminergic nigrostriatal pathway in parkinsonian rhesus monkeys. *Hum Gene Ther*. 2009; 20(5):511–8. Epub 2009/03/04. doi: [10.1089/hum.2008.201](#) PMID: [19254173](#)
24. Kells AP, Eberling J, Su X, Pivrotto P, Bringas J, Hadaczek P, et al. Regeneration of the MPTP-lesioned dopaminergic system after convection-enhanced delivery of AAV2-GDNF. *J Neurosci*. 2010; 30(28):9567–77. Epub 2010/07/16. doi: [10.1523/JNEUROSCI.0942-10.2010](#) PMID: [20631185](#)
25. Lo Bianco C, Deglon N, Pralong W, Aebischer P. Lentiviral nigral delivery of GDNF does not prevent neurodegeneration in a genetic rat model of Parkinson's disease. *Neurobiol Dis*. 2004; 17(2):283–9. Epub 2004/10/12. PMID: [15474365](#)
26. Decressac M, Ulusoy A, Mattsson B, Georgievska B, Romero-Ramos M, Kirik D, et al. GDNF fails to exert neuroprotection in a rat alpha-synuclein model of Parkinson's disease. *Brain: a journal of neurology*. 2011; 134(Pt 8):2302–11. Epub 2011/06/30.
27. Decressac M, Kadkhodaei B, Mattsson B, Laguna A, Perlmann T, Bjorklund A. alpha-Synuclein-induced down-regulation of Nurr1 disrupts GDNF signaling in nigral dopamine neurons. *Sci Transl Med*. 2012; 4(163):163ra56. Epub 2012/12/12.
28. Olanow CW. Parkinson disease: Gene therapy for Parkinson disease—a hope, or a dream? *Nat Rev Neurol*. 2014; 10(4):186–7. Epub 2014/03/26. doi: [10.1038/nrneurol.2014.45](#) PMID: [24662536](#)
29. Gill SS, Patel NK, Hotton GR, O'Sullivan K, McCarter R, Bunnage M, et al. Direct brain infusion of glial cell line-derived neurotrophic factor in Parkinson disease. *Nat Med*. 2003; 9(5):589–95. Epub 2003/04/02. PMID: [12669033](#)
30. Nutt JG, Burchiel KJ, Comella CL, Jankovic J, Lang AE, Laws ER Jr., et al. Randomized, double-blind trial of glial cell line-derived neurotrophic factor (GDNF) in PD. *Neurology*. 2003; 60(1):69–73. Epub 2003/01/15. PMID: [12525720](#)
31. Slevin JT, Gerhardt GA, Smith CD, Gash DM, Kryscio R, Young B. Improvement of bilateral motor functions in patients with Parkinson disease through the unilateral intraputamenal infusion of glial cell line-derived neurotrophic factor. *J Neurosurg*. 2005; 102(2):216–22. Epub 2005/03/03. PMID: [15739547](#)
32. Lang AE, Gill S, Patel NK, Lozano A, Nutt JG, Penn R, et al. Randomized controlled trial of intraputamenal glial cell line-derived neurotrophic factor infusion in Parkinson disease. *Ann Neurol*. 2006; 59(3):459–66. Epub 2006/01/24. PMID: [16429411](#)
33. Sherer TB, Fiske BK, Svendsen CN, Lang AE, Langston JW. Crossroads in GDNF therapy for Parkinson's disease. *Movement Disorders*. 2006; 21(2):136–41. PMID: [16470786](#)
34. Gimenez F, Krauze MT, Valles F, Hadaczek P, Bringas J, Sharma N, et al. Image-guided convection-enhanced delivery of GDNF protein into monkey putamen. *Neuroimage*. 2011; 54 Suppl 1:S189–95. Epub 2010/01/19. doi: [10.1016/j.neuroimage.2010.01.023](#) PMID: [20080195](#)
35. Richardson RM, Kells AP, Rosenbluth KH, Salegio EA, Fiandaca MS, Larson PS, et al. Interventional MRI-guided putamenal delivery of AAV2-GDNF for a planned clinical trial in Parkinson's disease. *Mol Ther*. 2011; 19(6):1048–57. Epub 2011/02/24. doi: [10.1038/mt.2011.11](#) PMID: [21343917](#)
36. Yin D, Forsayeth J, Bankiewicz KS. Optimized cannula design and placement for convection-enhanced delivery in rat striatum. *J Neurosci Methods*. 2010; 187(1):46–51. Epub 2009/12/23. doi: [10.1016/j.jneumeth.2009.12.008](#) PMID: [20026357](#)
37. Ramaswamy S, Soderstrom KE, Kordower JH. Trophic factors therapy in Parkinson's disease. *Prog Brain Res*. 2009; 175:201–16. Epub 2009/08/08. doi: [10.1016/S0079-6123\(09\)17514-3](#) PMID: [19660658](#)
38. Bepalov MM, Sidorova YA, Tumova S, Ahonen-Bishopp A, Magalhaes AC, Kuleskiy E, et al. Heparan sulfate proteoglycan syndecan-3 is a novel receptor for GDNF, neurturin, and artemin. *J Cell Biol*. 2011; 192(1):153–69. Epub 2011/01/05. doi: [10.1083/jcb.201009136](#) PMID: [21200028](#)
39. Hamilton JF, Morrison PF, Chen MY, Harvey-White J, Pernaute RS, Phillips H, et al. Heparin coinfusion during convection-enhanced delivery (CED) increases the distribution of glial-derived neurotrophic factor (GDNF) ligand family in rat striatum and enhances the pharmacological activity of neurturin. *Exp Neurol*. 2001; 168(1): 155–61. PMID: [11170730](#)
40. Day-Lollini PA, Stewart GR, Taylor MJ, Johnson RM, Chellman GJ. Hyperplastic changes within the leptomeninges of the rat and monkey in response to chronic intracerebroventricular infusion of nerve growth factor. *Exp Neurol*. 1997; 145(1):24–37. Epub 1997/05/01. PMID: [9184106](#)
41. Kordower JH, Emborg ME, Bloch J, Ma SY, Chu Y, Leventhal L, et al. Neurodegeneration prevented by lentiviral vector delivery of GDNF in primate models of Parkinson's disease. *Science*. 2000; 290(5492):767–73. Epub 2000/10/29. PMID: [11052933](#)

42. Hovland DN Jr., Boyd RB, Butt MT, Engelhardt JA, Moxness MS, Ma MH, et al. Six-month continuous intraputamenal infusion toxicity study of recombinant methionyl human glial cell line-derived neurotrophic factor (r-metHuGDNF in rhesus monkeys. *Toxicol Pathol.* 2007; 35(7):1013–29. Epub 2007/12/22. PMID: [18098052](#)
43. Stanic D, Finkelstein DI, Bourke DW, Drago J, Horne MK. Timecourse of striatal re-innervation following lesions of dopaminergic SNpc neurons of the rat. *Eur J Neurosci.* 2003; 18(5):1175–88. PMID: [12956716](#)
44. Henderson JM, Stanic D, Tomas D, Patch J, Horne MK, Bourke D, et al. Postural changes after lesions of the substantia nigra pars reticulata in hemiparkinsonian monkeys. *Behavioural brain research.* 2005; 160(2):267–76. Epub 2005/05/03. PMID: [15863223](#)
45. Eslamboli A, Georgievska B, Ridley RM, Baker HF, Muzyczka N, Burger C, et al. Continuous low-level glial cell line-derived neurotrophic factor delivery using recombinant adeno-associated viral vectors provides neuroprotection and induces behavioral recovery in a primate model of Parkinson's disease. *J Neurosci.* 2005; 25(4):769–77. Epub 2005/01/28. PMID: [15673656](#)
46. Duty S, Jenner P. Animal models of Parkinson's disease: a source of novel treatments and clues to the cause of the disease. *British Journal of Pharmacology.* 2011; 164(4):1357–91. doi: [10.1111/j.1476-5381.2011.01426.x](#) PMID: [21486284](#)
47. Lee J, Zhu WM, Stanic D, Finkelstein DI, Horne MH, Henderson J, et al. Sprouting of dopamine terminals and altered dopamine release and uptake in Parkinsonian dyskinesia. *Brain.* 2008; 131(6):1574–87. Epub 2008/05/20.
48. Franke SK, van Kesteren RE, Wubben JA, Hofman S, Paliukhovich I, van der Schors RC, et al. Progression and recovery of Parkinsonism in a chronic progressive MPTP-induction model in the marmoset without persistent molecular and cellular damage. *Neuroscience.* 2016; 312:247–59. Epub 2015/10/04. doi: [10.1016/j.neuroscience.2015.09.065](#) PMID: [26431624](#)
49. Garea-Rodriguez E, Schlumbohm C, Czeh B, Konig J, Helms G, Heckmann C, et al. Visualizing dopamine transporter integrity with iodine-123-FP-CIT SPECT in combination with high resolution MRI in the brain of the common marmoset monkey. *J Neurosci Methods.* 2012; 210(2):195–201. Epub 2012/07/26. doi: [10.1016/j.jneumeth.2012.07.009](#) PMID: [22827895](#)
50. Stephan H, Baron G, Schwedtfeger WK. *The brain of the common marmoset (Callithrix jacchus): a stereotaxic atlas.* Berlin; New York: Springer-Verlag; 1980.
51. Helms G, Garea-Rodriguez E, Schlumbohm C, Konig J, Dechent P, Fuchs E, et al. Structural and quantitative neuroimaging of the common marmoset monkey using a clinical MRI system. *J Neurosci Methods.* 2013; 215(1):121–31. Epub 2013/03/12. doi: [10.1016/j.jneumeth.2013.02.011](#) PMID: [23473795](#)
52. Jack CR Jr., Bernstein MA, Fox NC, Thompson P, Alexander G, Harvey D, et al. The Alzheimer's Disease Neuroimaging Initiative (ADNI): MRI methods. *J Magn Reson Imaging.* 2008; 27(4):685–91. Epub 2008/02/28. doi: [10.1002/jmri.21049](#) PMID: [18302232](#)
53. Yuasa S, Nakamura K, Kohsaka S. *Stereotaxic atlas of the marmoset brain.* Tokyo: National Institute of Neuroscience; 2009.
54. Sun ZP, Gong L, Huang SH, Geng Z, Cheng L, Chen ZY. Intracellular trafficking and secretion of cerebral dopamine neurotrophic factor in neurosecretory cells. *J Neurochem.* 2011; 117(1):121–32. Epub 2011/01/18. doi: [10.1111/j.1471-4159.2011.07179.x](#) PMID: [21235575](#)
55. Lindstrom R, Lindholm P, Kallijarvi J, Yu LY, Piepponen TP, Arumae U, et al. Characterization of the structural and functional determinants of MANF/CDNF in *Drosophila* in vivo model. *PLoS One.* 2013; 8(9):e73928. Epub 2013/09/11. doi: [10.1371/journal.pone.0073928](#) PMID: [24019940](#)
56. Raykhel I, Alanen H, Salo K, Jurvansuu J, Nguyen VD, Latva-Ranta M, et al. A molecular specificity code for the three mammalian KDEL receptors. *J Cell Biol.* 2007; 179(6):1193–204. Epub 2007/12/19. PMID: [18086916](#)
57. Eslamboli A, Cummings RM, Ridley RM, Baker HF, Muzyczka N, Burger C, et al. Recombinant adeno-associated viral vector (rAAV) delivery of GDNF provides protection against 6-OHDA lesion in the common marmoset monkey (*Callithrix jacchus*). *Exp Neurol.* 2003; 184(1):536–48. Epub 2003/11/26. PMID: [14637123](#)
58. Grondin R, Zhang Z, Yi A, Cass WA, Maswood N, Andersen AH, et al. Chronic, controlled GDNF infusion promotes structural and functional recovery in advanced parkinsonian monkeys. *Brain.* 2002; 125(Pt 10):2191–201. Epub 2002/09/24. PMID: [12244077](#)
59. Kordower JH, Palfi S, Chen EY, Ma SY, Sendera T, Cochran EJ, et al. Clinicopathological findings following intraventricular glial-derived neurotrophic factor treatment in a patient with Parkinson's disease. *Ann Neurol.* 1999; 46(3):419–24. Epub 1999/09/11. PMID: [10482276](#)
60. Booi J, de Bruin K, Habraken JB, Voorn P. Imaging of dopamine transporters in rats using high-resolution pinhole single-photon emission tomography. *Eur J Nucl Med Mol Imaging.* 2002; 29(9):1221–4. Epub 2002/11/07. PMID: [12418461](#)

61. Andringa G, Drukarch B, Bol JG, de Bruin K, Sorman K, Habraken JB, et al. Pinhole SPECT imaging of dopamine transporters correlates with dopamine transporter immunohistochemical analysis in the MPTP mouse model of Parkinson's disease. *Neuroimage*. 2005; 26(4):1150–8. Epub 2005/05/24. PMID: [15908232](#)
62. Saji H, Iida Y, Kawashima H, Ogawa M, Kitamura Y, Mukai T, et al. In vivo imaging of brain dopaminergic neurotransmission system in small animals with high-resolution single photon emission computed tomography. *Anal Sci*. 2003; 19(1):67–71. Epub 2003/02/01. PMID: [12558026](#)
63. Alvarez-Fischer D, Blessmann G, Trosowski C, Behe M, Schurrat T, Hartmann A, et al. Quantitative [(123)I]FP-CIT pinhole SPECT imaging predicts striatal dopamine levels, but not number of nigral neurons in different mouse models of Parkinson's disease. *Neuroimage*. 2007; 38(1):5–12. Epub 2007/08/25. PMID: [17716921](#)
64. Seibyl JP, Marek K, Sheff K, Zoghbi S, Baldwin RM, Charney DS, et al. Iodine-123-beta-CIT and iodine-123-FPCIT SPECT measurement of dopamine transporters in healthy subjects and Parkinson's patients. *J Nucl Med*. 1998; 39(9):1500–8. Epub 1998/09/23. PMID: [9744331](#)
65. de la Fuente-Fernandez R. Role of DaTSCAN and clinical diagnosis in Parkinson disease. *Neurology*. 78(10):696–701. Epub 2012/02/11. doi: [10.1212/WNL.0b013e318248e520](#) PMID: [22323748](#)
66. Porritt MJ, Batchelor PE, Hughes AJ, Kalnins R, Donnan GA, Howells DW. New dopaminergic neurons in Parkinson's disease striatum. *Lancet*. 2000; 356(9223):44–5. Epub 2000/07/13. PMID: [10892768](#)
67. Palfi S, Leventhal L, Chu Y, Ma SY, Emborg M, Bakay R, et al. Lentivirally delivered glial cell line-derived neurotrophic factor increases the number of striatal dopaminergic neurons in primate models of nigrostriatal degeneration. *J Neurosci*. 2002; 22(12):4942–54. Epub 2002/06/22. PMID: [12077191](#)
68. Kirik D, Rosenblad C, Bjorklund A, Mandel RJ. Long-term rAAV-mediated gene transfer of GDNF in the rat Parkinson's model: intrastriatal but not intranigral transduction promotes functional regeneration in the lesioned nigrostriatal system. *J Neurosci*. 2000; 20(12):4686–700. PMID: [10844038](#)
69. Schober A. Classic toxin-induced animal models of Parkinson's disease: 6-OHDA and MPTP. *Cell Tissue Res*. 2004; 318(1):215–24. PMID: [15503155](#)
70. Blanchard V, Anglade P, Dziejczapolski G, Savasta M, Agid Y, Raisman-Vozari R. Dopaminergic sprouting in the rat striatum after partial lesion of the substantia nigra. *Brain Res*. 1996; 709(2):319–25. PMID: [8833770](#)
71. Onn SP, Berger TW, Stricker EM, Zigmond MJ. Effects of intraventricular 6-hydroxydopamine on the dopaminergic innervation of striatum: histochemical and neurochemical analysis. *Brain Res*. 1986; 376(1):8–19. Epub 1986/06/18. PMID: [3087584](#)
72. Kirik D, Annett LE, Burger C, Muzyczka N, Mandel RJ, Bjorklund A. Nigrostriatal alpha-synucleinopathy induced by viral vector-mediated overexpression of human alpha-synuclein: a new primate model of Parkinson's disease. *Proc Natl Acad Sci USA*. 2003; 100(5):2884–9. Epub 2003/02/24. PMID: [12601150](#)
73. Eslamboli A, Romero-Ramos M, Burger C, Bjorklund T, Muzyczka N, Mandel RJ. *Brain*. 2007; 130(3):799–815. Epub 2007/02/15.
74. Latge C, Cabral KM, de Oliveira GA, Raymundo DP, Freitas JA, Johanson L, et al. The Solution Structure and Dynamics of Full-length Human Cerebral Dopamine Neurotrophic Factor and Its Neuroprotective Role against alpha-Synuclein Oligomers. *J Biol Chem*. 2015; 290(33):20527–40. Epub 2015/07/08. doi: [10.1074/jbc.M115.662254](#) PMID: [26149686](#)
75. Glembotski CC, Thuerauf DJ, Huang C, Vekich JA, Gottlieb RA, Doroudgar S. Mesencephalic astrocyte-derived neurotrophic factor protects the heart from ischemic damage and is selectively secreted upon sarco/endoplasmic reticulum calcium depletion. *J Biol Chem*. 2012; 287(31):25893–904. Epub 2012/05/29. doi: [10.1074/jbc.M112.356345](#) PMID: [22637475](#)
76. Henderson MJ, Richie CT, Airavaara M, Wang Y, Harvey BK. Mesencephalic astrocyte-derived neurotrophic factor (MANF) secretion and cell surface binding are modulated by KDEL receptors. *J Biol Chem*. 2013; 288(6):4209–25. Epub 2012/12/21. doi: [10.1074/jbc.M112.400648](#) PMID: [23255601](#)